Electronic Supplementary Material (ESI) for Journal of Materials Chemistry C.

Regulating the color output and simultaneously enhancing the intensity of upconversion nanoparticles *via* dye-sensitized strategy

Bin Xue, ‡ [a,b] Dan Wang, ‡ [a] Youlin Zhang,[b] Jing Zuo,[b] Yulei Chang,[b] LangpingTu,*[b] Xiaomin Liu,[c] Zhen Yuan,[d] Huiying Zhao,[e] Jun Song, *[a] Junle Qu, *[a] Xianggui Kong,*[b]

[a] Key Laboratory of Optoelectronic Devices and Systems of Ministry of Education and Guangdong Province, College of Physics and Optoelectronic Engineering, Shenzhen University, Shenzhen 518060, P. R. China

[b] State Key Laboratory of Luminescence and Applications, Changchun Institute of Optics, Fine Mechanics and Physics, Chinese Academy of Sciences,130033 Changchun, China.

[c] State Key Laboratory on Integrated Optoelectronics, College of Electronic Science and Engineering, Jilin University, Changchun 130012, People's Republic of China

[d] Bioimaging Core, Faculty of Health Sciences, University of Macau, Macao, China

[e] The First Hospital, Jilin University, Changchun 130021, P. R. China

‡These authors contributed equally.

Part I. Supporting Data.

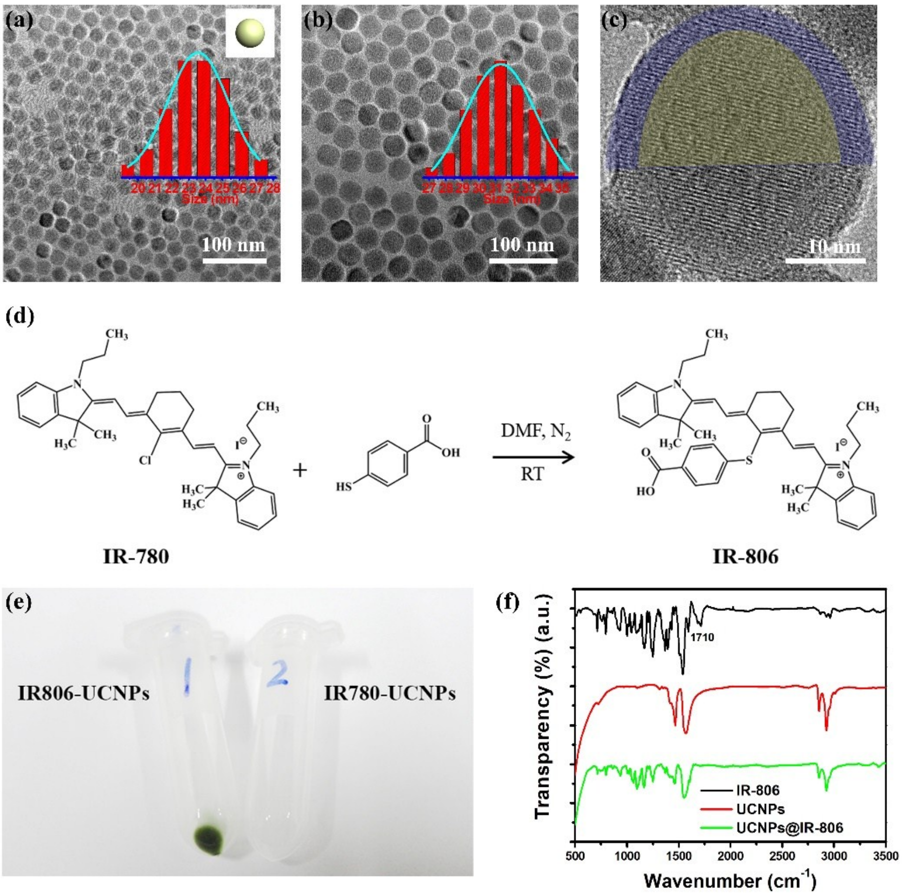

Fig. S1 (a) $NaYF_4$:Yb/Er (25/2%) nanoparticles (core, ~23.9±1.9 nm) and (b) $NaYF_4$:Yb/Er (25/2%)@ $NaYF_4$: Nd(20%) nanoparticles (core-shell, ~31.3±1.5 nm). (c) HRTEM image of the corresponding core-shell nanoparticles. (d) Synthesis process of IR-806. (e) Centrifugation results of binding of IR-806 (left) and IR-780 (right) to the nanoparticles. IR-806 can coordinate with UCNPs through the carboxyl group. Successful synthesis of IR-806 was confirmed by the absorption peak shifted from 780 nm to 806 nm (Fig. S4) and the NMR spectra (Fig. S5). After the dye-conjugating process, IR-806, rather than IR-780, could attach UCNPs, which can be directly observed from the color changes after centrifuged the mixed solutions of dyes and UCNPs. Moreover, the absorption spectra and excitation spectra of IR-806 were also kept ~ 800 nm after conjugated on the surface of UCNPs (Fig. S6 and S7). (f) FTIR spectra of IR-806 (black line), UCNPs (red line), IR-806 conjugated UCNPs (green line). After IR-806 conjugating on the surface of UCNPs, the mixtures generated many FTIR peaks ranged from 1000 to 1500 cm^{-1}, which arose from IR-806. Moreover, due to IR-806 coordinate with UCNPs through the carboxyl group, the vibration mode of the carboxyl group (1710 cm^{-1}) was disappeared due to the coordination interaction with nanoparticles. All these results demonstrated that dyes IR-806 successfully conjugated on the surface of UCNPs.

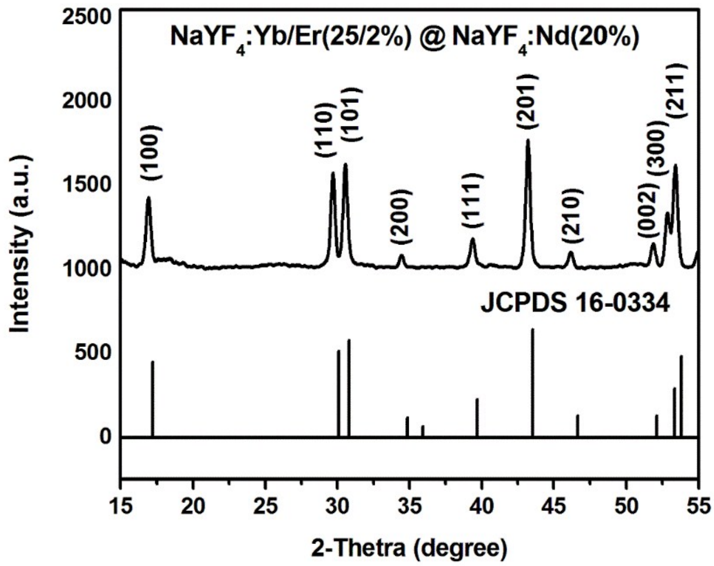

Fig. S2 XRD diffraction pattern of the standard reference pattern β-$NaYF_4$ (JCPDS-16-0334, bottom) and the synthesized $NaYF_4$:Yb/Er(25/2%) @ $NaYF_4$:Nd(20%) nanoparticles.

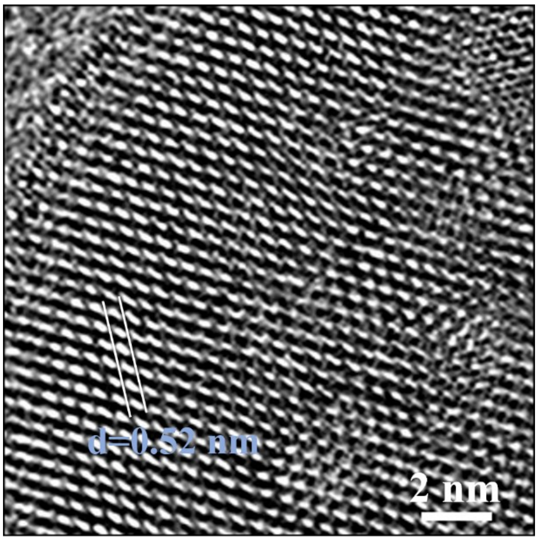

Fig. S3 High-resolution TEM of the $NaYF_4$:Yb/Er (25/2%)@$NaYF_4$:Nd (20%) upconversion nanoparticles, the typical d-spacing of lattice was about 0.52 nm, which corresponded to the (100) plane of the hexagonal $NaYF_4$ phase.

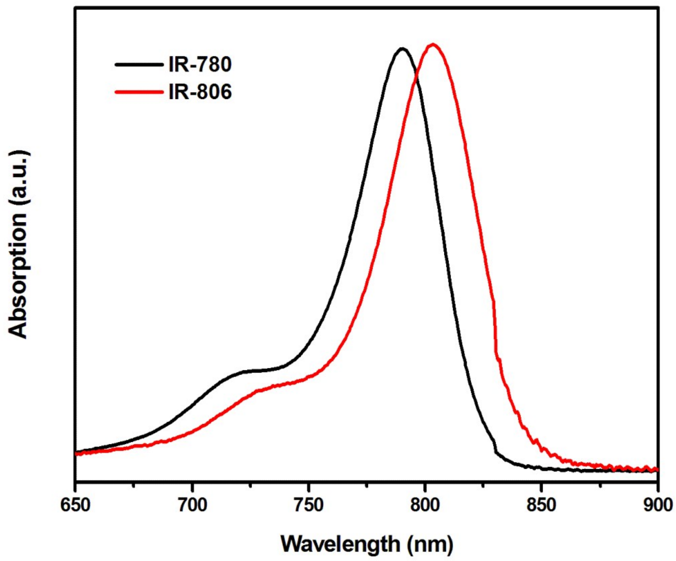

Fig. S4 Absorption spectra of IR-780 (black line) and carboxylic acid derivative IR-806 (red line) in $CHCl_3$.

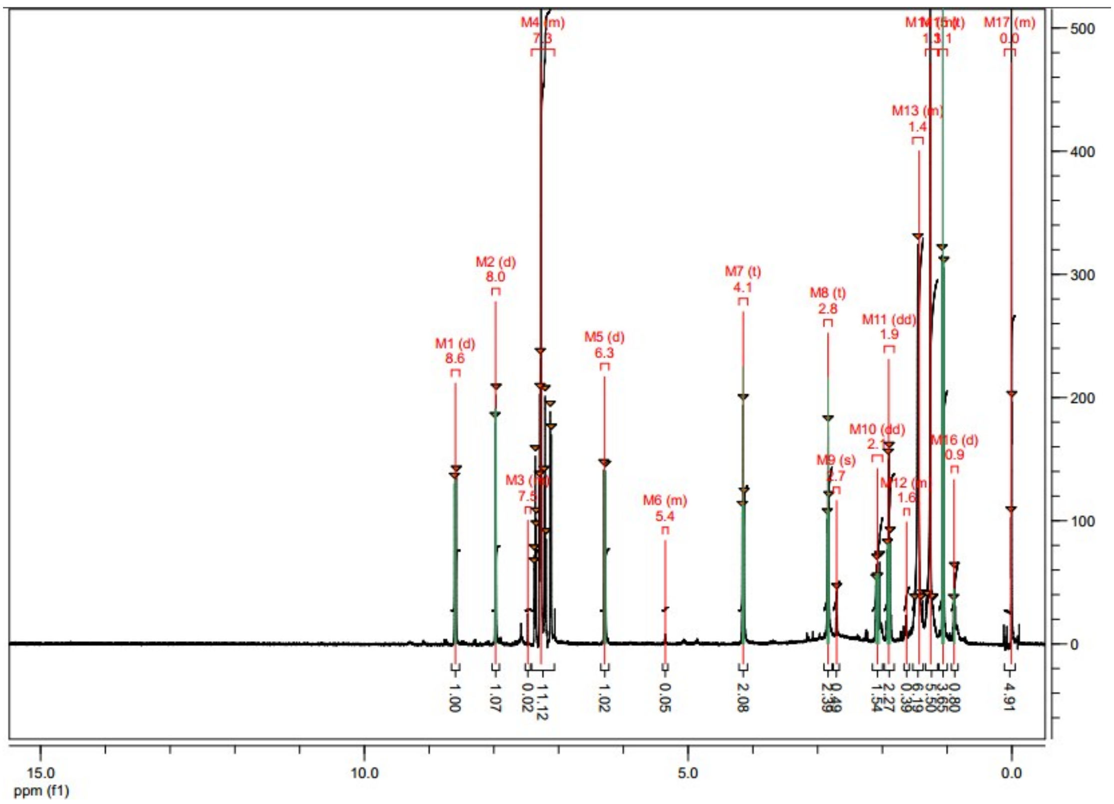

Fig. S5 ^{1}H-NMR (500 MHz, $CDCl_3$) spectrum of IR-806.

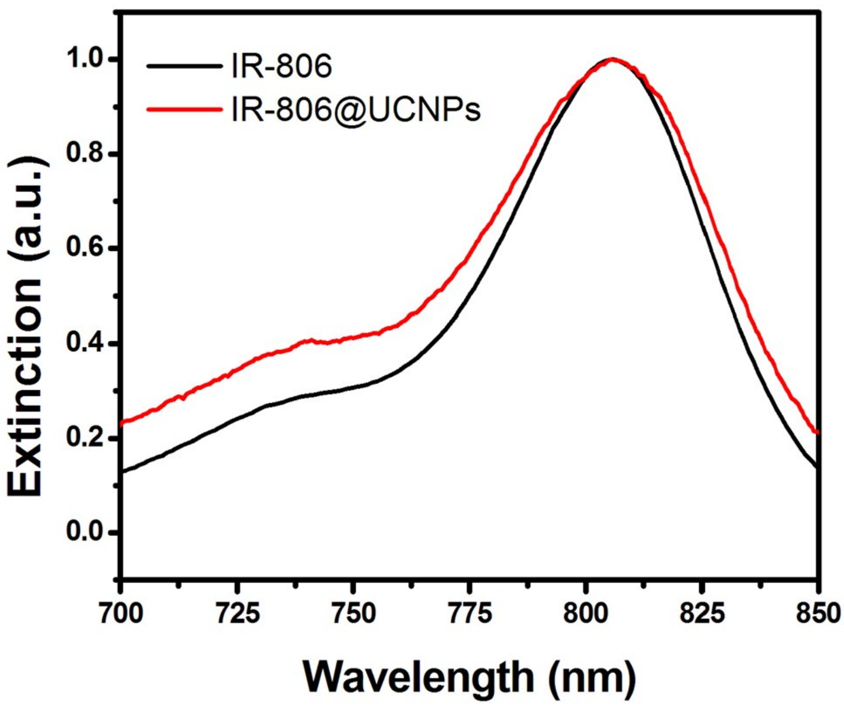

Fig. S6 Absorption spectra of IR-806 (black line) and dye-sensitized $NaYF_4$: Yb/Er (25/2%)@ $NaYF_4$: Nd(20%) nanoparticles (red line).

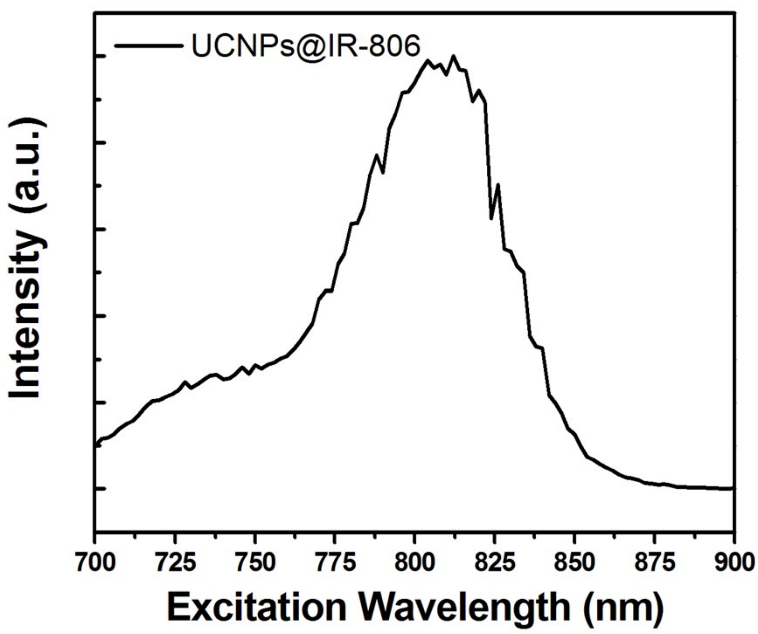

Fig. S7 Excitation spectra of IR-806 after conjugated on UCNPs, the monitored emission wavelength was kept 830 nm.

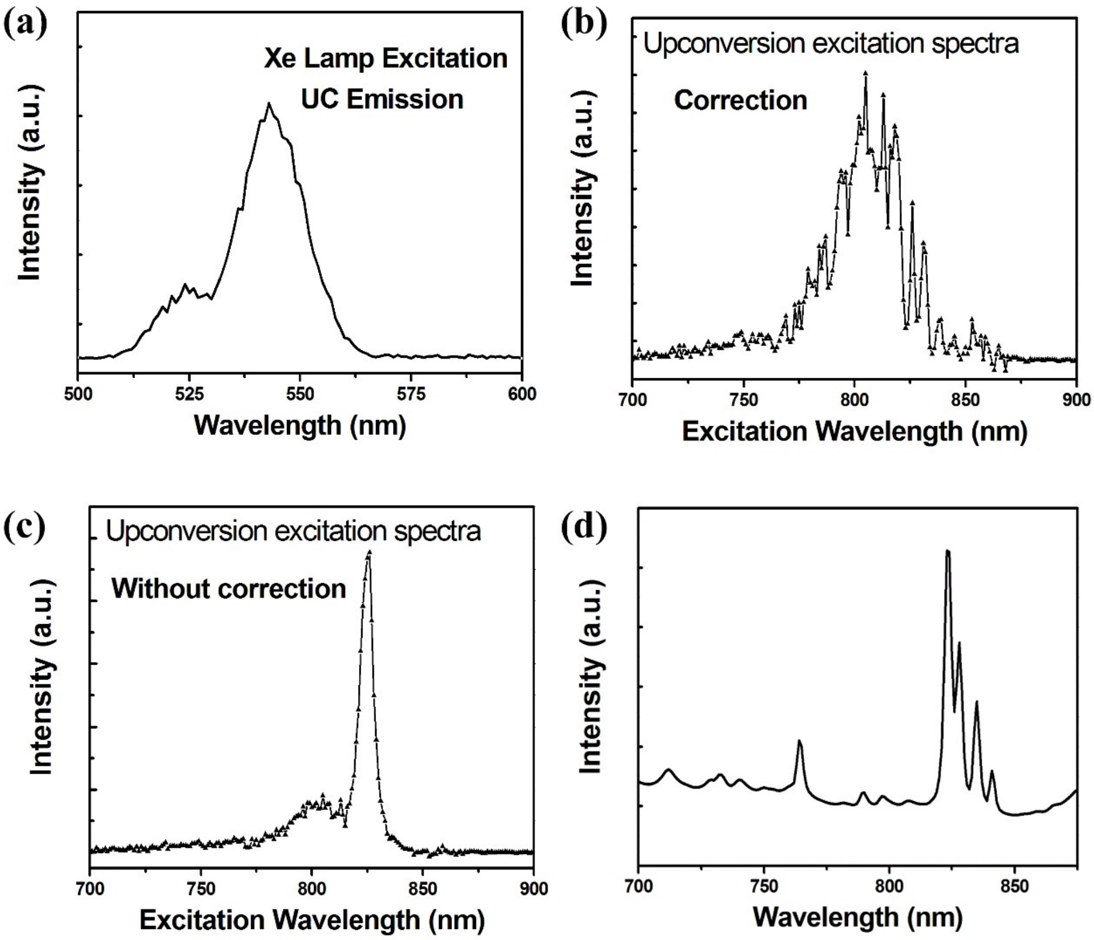

Fig. S8 (a) UCL of the IR-806 sensitized core-shell UCNPs under excitation of Xe lamp (excitation wavelength ~800 nm, ~ 1mW/cm^2), (b) the corrected upconversion excitation spectra of the IR-806 sensitized core-shell UCNPs, (c) upconversion excitation spectra of the IR-806 sensitized core-shell UCNPs without correction. (d) Emission spectra of the Xe lamp. Due to the IR-sensitized UCNPs could be excited by Xe lamp (a), the upconversion excitation spectra could be obtained, as shown in (b). It should be noted that the upconversion excitation spectra should be corrected. Without correction (c), some inference peak would appear. In the FLS980 system, the excitation spectra can be obtained as: $E_{ex}(\lambda)=I_{em}(\lambda)/I_{ref\ lamp}(\lambda)=k(\lambda)$, where k(λ) is a ratio constant at different wavelength position. For upconversion, $I_{em}(\lambda)=k(\lambda)(I_{ref\ lamp}(\lambda))^n$, where n>1, which indicates a main multi-photon emission process. Then the the excitation spectra can be obtained as: $E_{excitation}(\lambda)= I_{emission}(\lambda)/I_{ref\ lamp}(\lambda)=k(\lambda)(I_{ref\ lamp}(\lambda))^n/I_{ref\ lamp}(\lambda) = k(\lambda)(I_{ref\ lamp}(\lambda))^{n-1}$. $I_{ref\ lamp}(\lambda)$ can be test the emission from the Xe lamp (d), n could be obtained from the log-log plots of the UCL intensity versus laser power densities, here n was 1.8, then the corrected upconversion spectra could be obtained in figure (b).

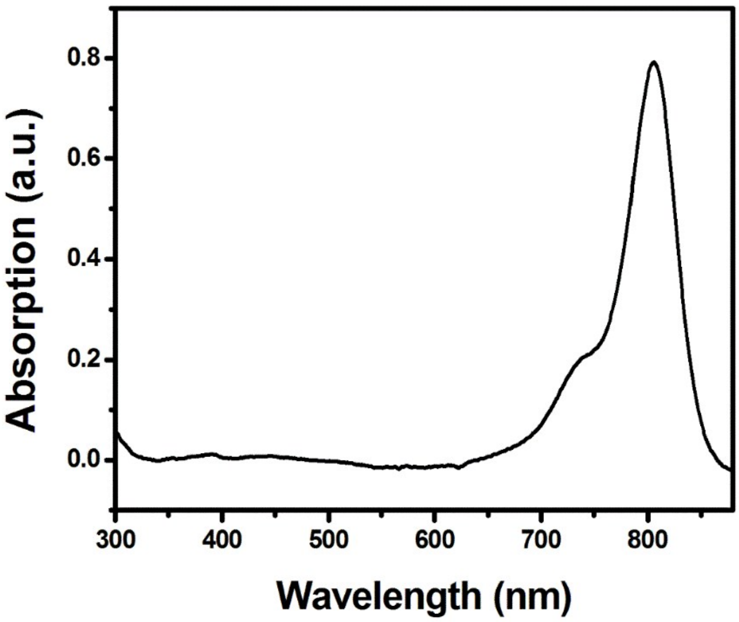

Fig. S9 Absorption spectra of IR-806 obtained in the whole visible range.

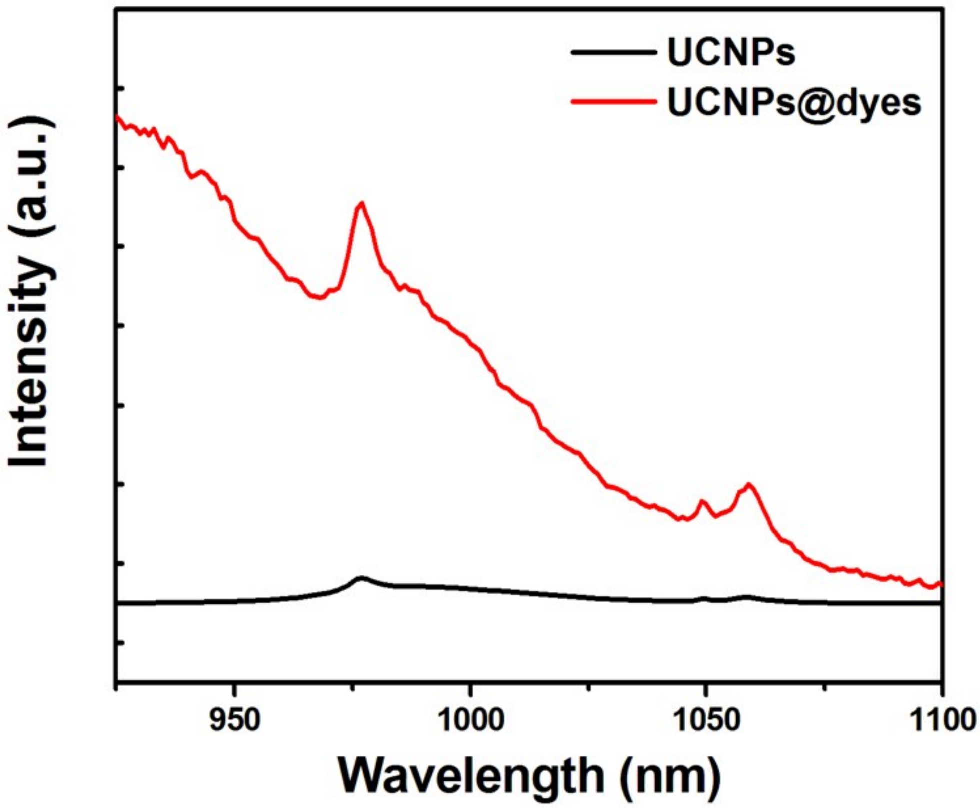

Fig. S10 The enhanced downconversion emission (~977 nm) of Yb^{3+} of $NaYF_4$:Yb/Er(25/2%) @ $NaYF_4$:Nd(20%) nanoparticles after dye-sensitization.

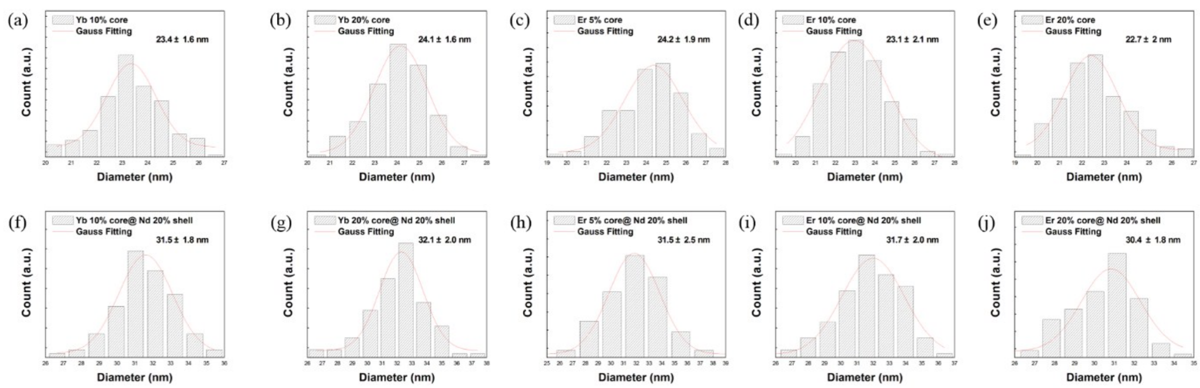

Fig. S11 The size distribution of (a) $NaYF_4$: Yb/Er (10/2%) nanoparticles, (b) $NaYF_4$: Yb/Er (20/2%) nanoparticles , (c) $NaYF_4$: Yb/Er (25/5%) nanoparticles , (d) $NaYF_4$: Yb/Er (25/10%) nanoparticles , (e) $NaYF_4$: Yb/Er (25/20%) nanoparticles , (f) $NaYF_4$:

Yb/Er (10/2%)@ $NaYF_4$: Nd(20%) nanoparticles , (g) $NaYF_4$: Yb/Er (20/2%)@ $NaYF_4$: Nd(20%) nanoparticles, (h) $NaYF_4$: Yb/Er (25/5%)@ $NaYF_4$: Nd(20%) nanoparticles, (i) $NaYF_4$: Yb/Er (25/10%)@ $NaYF_4$: Nd(20%) nanoparticles, (j) $NaYF_4$: Yb/Er (25/20%)@ $NaYF_4$: Nd(20%) nanoparticles.

.

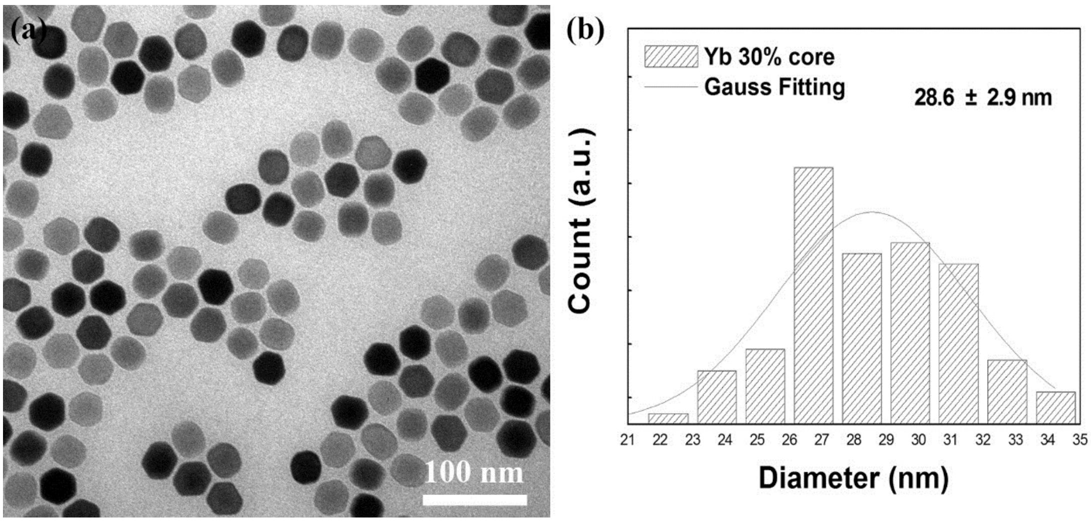

Fig. S12 (a) TEM images of $NaYF_4$: Yb/Er (30/2%) nanoparticles and (b) their size distribution.

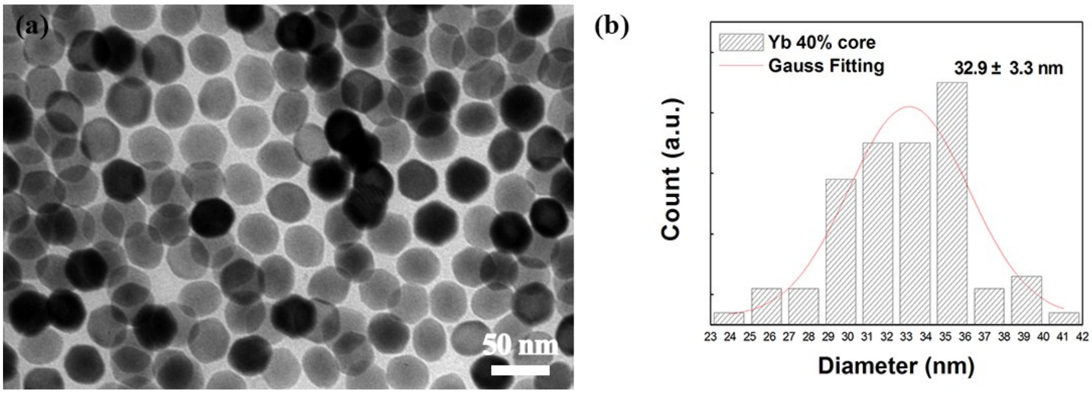

Fig. S13 (a) TEM image of $NaYF_4$: Yb/Er (40/2%) nanoparticles and (b) their size distribution.

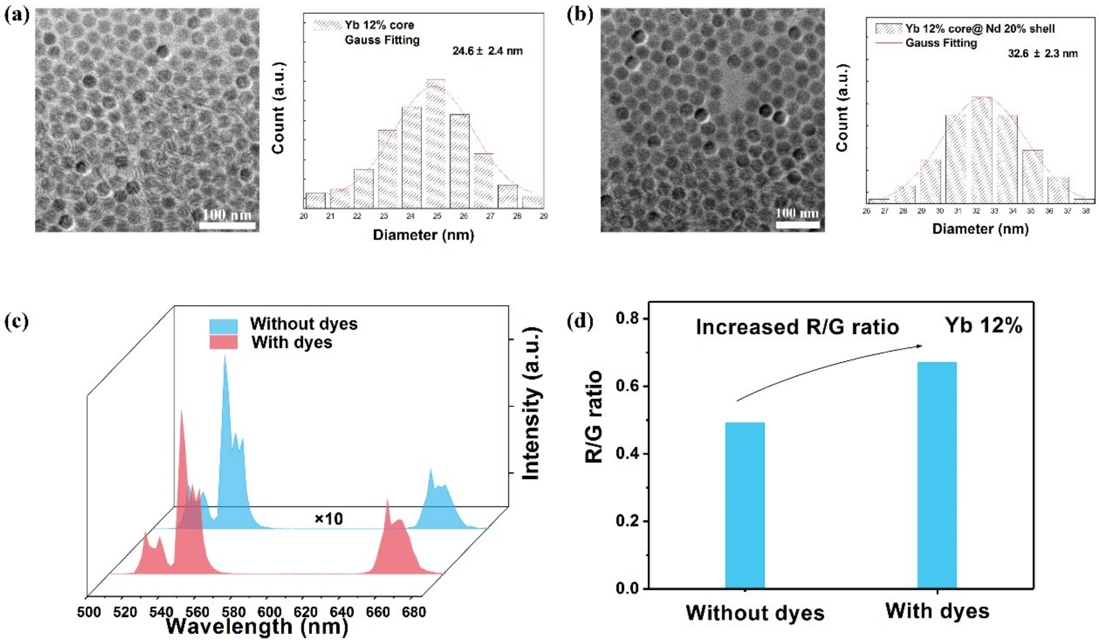

Fig. S14 (a) TEM image of $NaYF_4$: Yb/Er (12/2%) nanoparticles and their size distribution, (b) TEM image of $NaYF_4$: Yb/Er (12/2%)@ $NaYF_4$: Nd(20%) nanoparticles and their size distribution, (c) UCL spectra of $NaYF_4$: Yb/Er (12/2%)@ $NaYF_4$: Nd(20%) nanoparticles without or with dye sensitization under an excitation of 808 nm. (d) The changed R/G ratio of $NaYF_4$: Yb/Er (12/2%)@ $NaYF_4$: Nd(20%) nanoparticles after dye-sensitization.

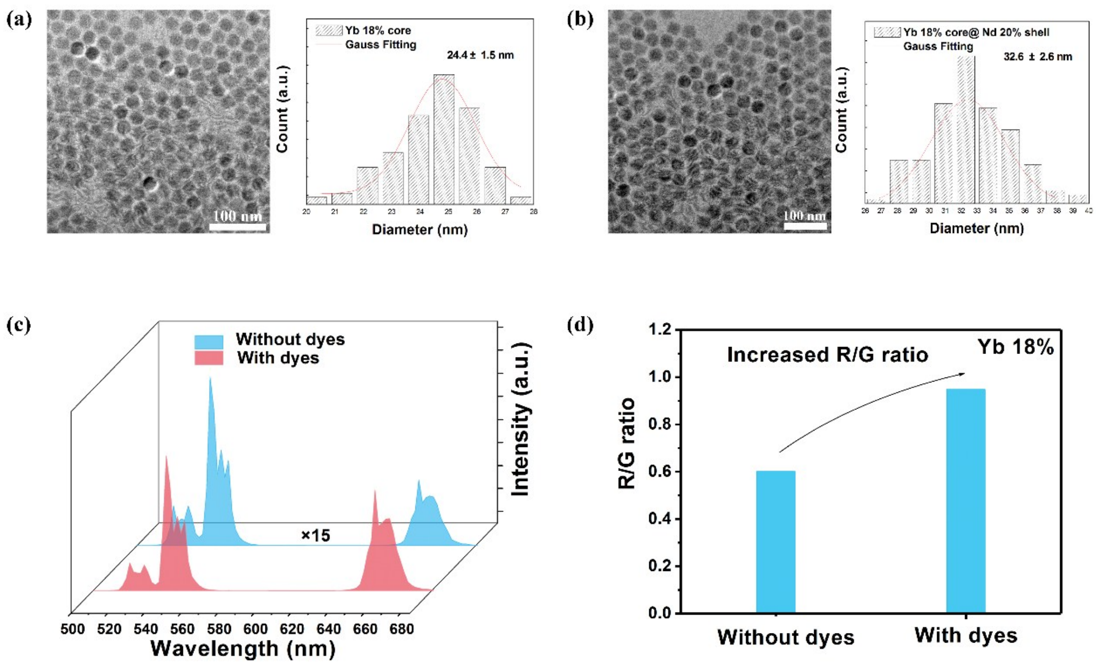

Fig. S15 (a) TEM image of $NaYF_4$: Yb/Er (18/2%) nanoparticles and their size distribution, (b) TEM image of $NaYF_4$: Yb/Er (18/2%)@ $NaYF_4$: Nd(20%) nanoparticles and their size distribution, (c) UCL spectra of $NaYF_4$: Yb/Er (18/2%)@ $NaYF_4$: Nd(20%) nanoparticles without or with dye sensitization under an excitation of 808 nm. (d) The changed R/G ratio of $NaYF_4$: Yb/Er (18/2%)@ $NaYF_4$: Nd(20%) nanoparticles after dye-sensitization.

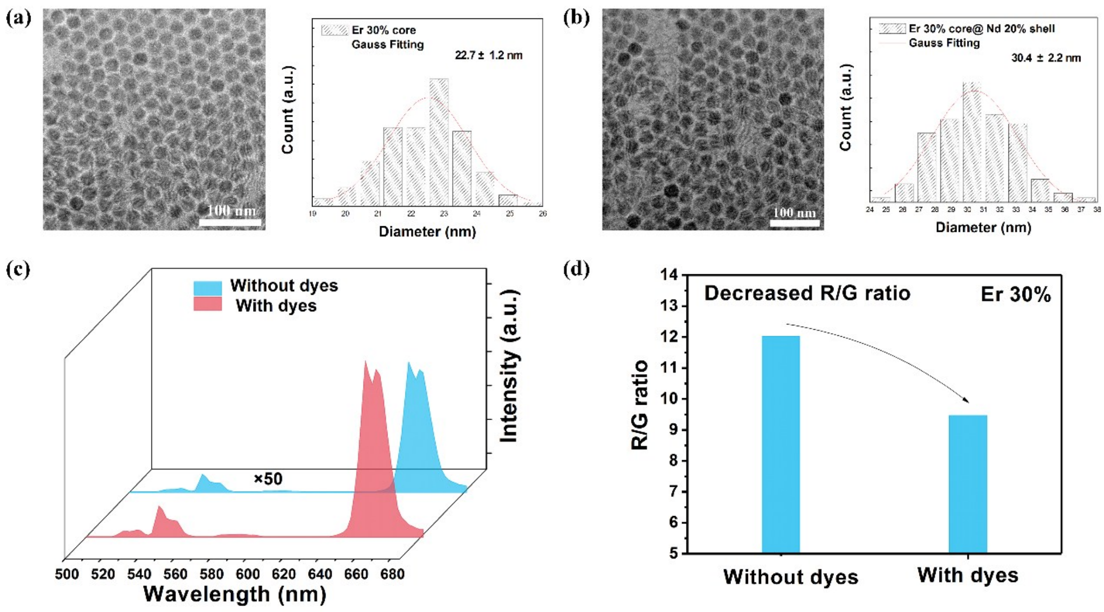

Fig. S16 (a) TEM image of $NaYF_4$: Yb/Er (25/30%) nanoparticles and their size distribution, (b) TEM image of $NaYF_4$: Yb/Er (25/30%)@ $NaYF_4$: Nd(20%) nanoparticles and their size distribution, (c) UCL spectra of $NaYF_4$: Yb/Er(25/30%)@ $NaYF_4$: Nd(20%) nanoparticles without or with dye sensitization under an excitation of 808 nm. (d) The changed R/G ratio of $NaYF_4$: Yb/Er (25/30%)@ $NaYF_4$: Nd(20%) nanoparticles after dye-sensitization.

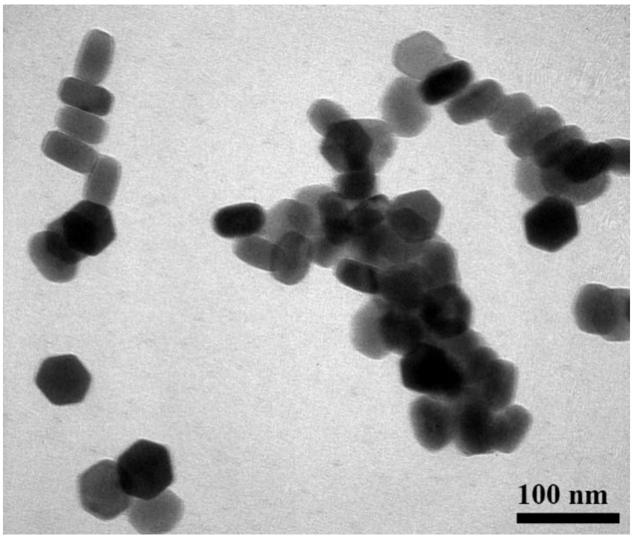

Fig. S17 TEM image of $NaYF_4$:Yb/Ho/Ce (10/2/10 %) @$NaYF_4$ nanoparticles

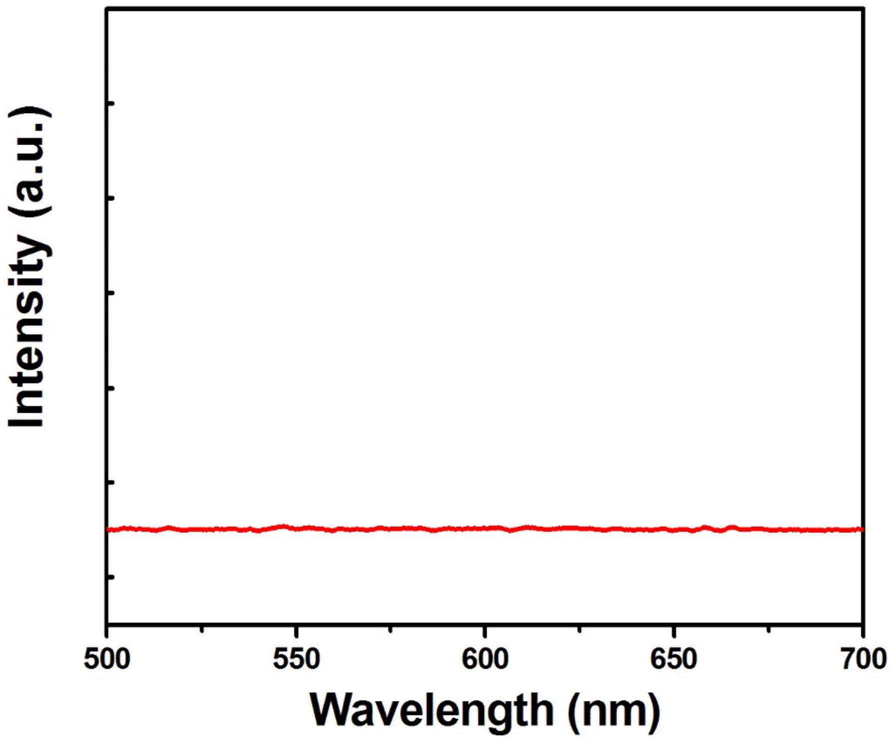

Fig. S18 UCL spectra of $NaYF_4$:Yb/Ho/Ce (10/2/10 %) @$NaYF_4$ nanoparticles under an excitation of 808 nm.

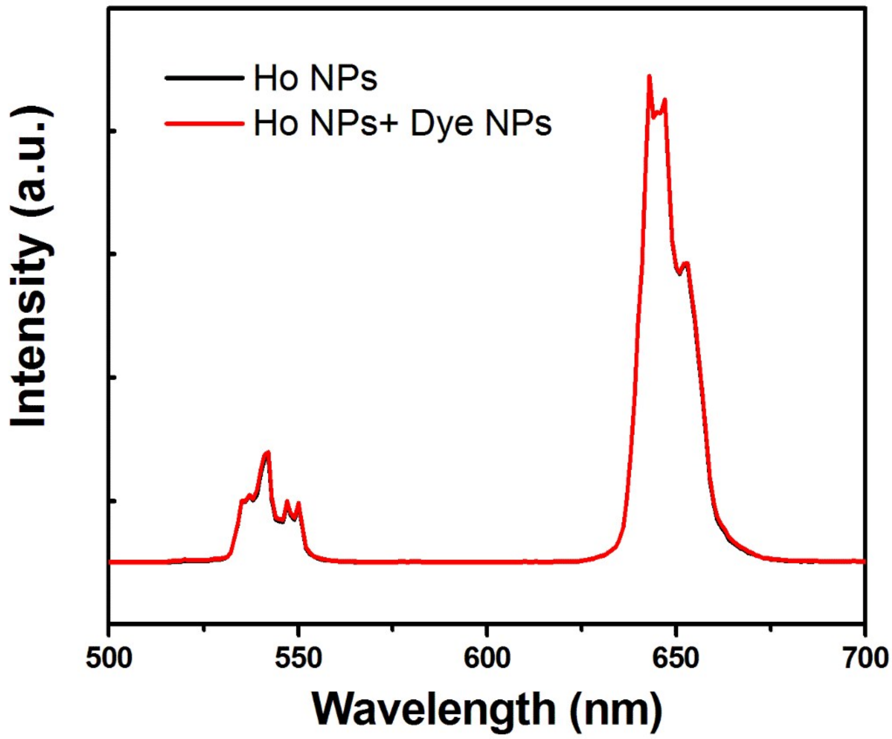

Fig. S19 UCL spectra of Ho-NPs (black line, ~20 mg/mL) and mixed solutions (red line, Ho-NPs (~20 mg/mL) + Dye-NPs (~0.5 mg/mL)) under an excitation of 980 nm.

Part II. Theory and Analysis.

Theory analysis of different upconversioin processes:

UC1:

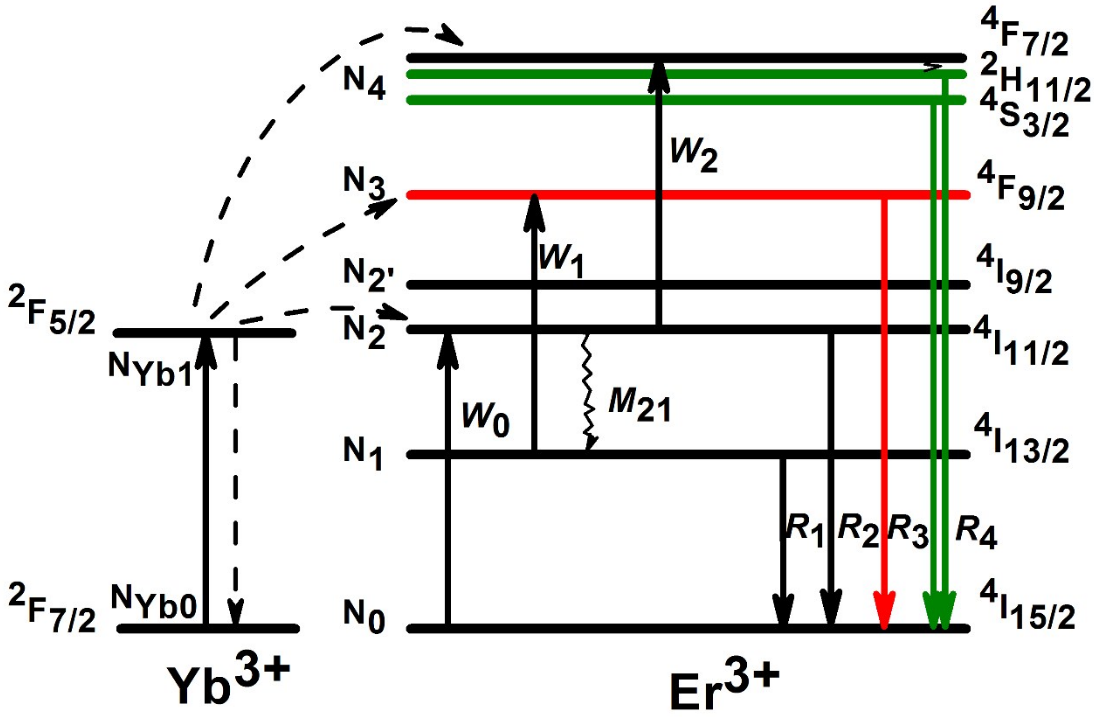

Fig. 20 Simplified energy-level diagrams illustrating the UC1 process.

$$\frac{dN_1}{dt} = M_{21}N_2 - W_1 N_{Yb1} N_1 - R_1 N_1 \quad (1)$$

$$\frac{dN_2}{dt} = W_0 N_{Yb1} N_0 - M_{21}N_2 - W_2 N_{Yb1} N_2 - R_2 N_2 \quad (2)$$

$$\frac{dN_3}{dt} = W_1 N_{Yb1} N_1 - R_3 N_3 \quad (3)$$

$$\frac{dN_4}{dt} = W_2 N_{Yb1} N_2 - R_4 N_4 \quad (4)$$

To solve the rate equations in stationary conditions, (1)~(4) convert to:

$$M_{21}N_2 - W_1 N_{Yb1} N_1 - R_1 N_1 = 0 \quad (5)$$

$$W_0 N_{Yb1} N_0 - M_{21}N_2 - W_2 N_{Yb1} N_2 - R_2 N_2 = 0 \quad (6)$$

$$W_1 N_{Yb1} N_1 - R_3 N_3 = 0 \quad (7)$$

$$W_2 N_{Yb1} N_2 - R_4 N_4 = 0 \quad (8)$$

According to (7), we obtain:

$$N_3 = \frac{W_1 N_{Yb1} N_1}{R_3} \quad (9)$$

According to (8), we obtain:

$$N_4 = \frac{W_2 N_{Yb1} N_2}{R_4} \quad (10)$$

Then, according to (9) and (10):

$$\frac{N_3}{N_4} = \frac{W_1 R_4 N_1}{W_2 R_3 N_2} \quad (11)$$

According to (5), we obtain:

$$\frac{N_1}{N_2} = \frac{M_{21}}{W_1 N_{Yb1} + R_1} \quad (12)$$

According to (11) and (12):

$$\frac{N_3}{N_4} = \frac{W_1 M_{21} R_4}{W_2 R_3 (R_1 + W_1 N_{Yb1})} \quad (13)$$

UC2:

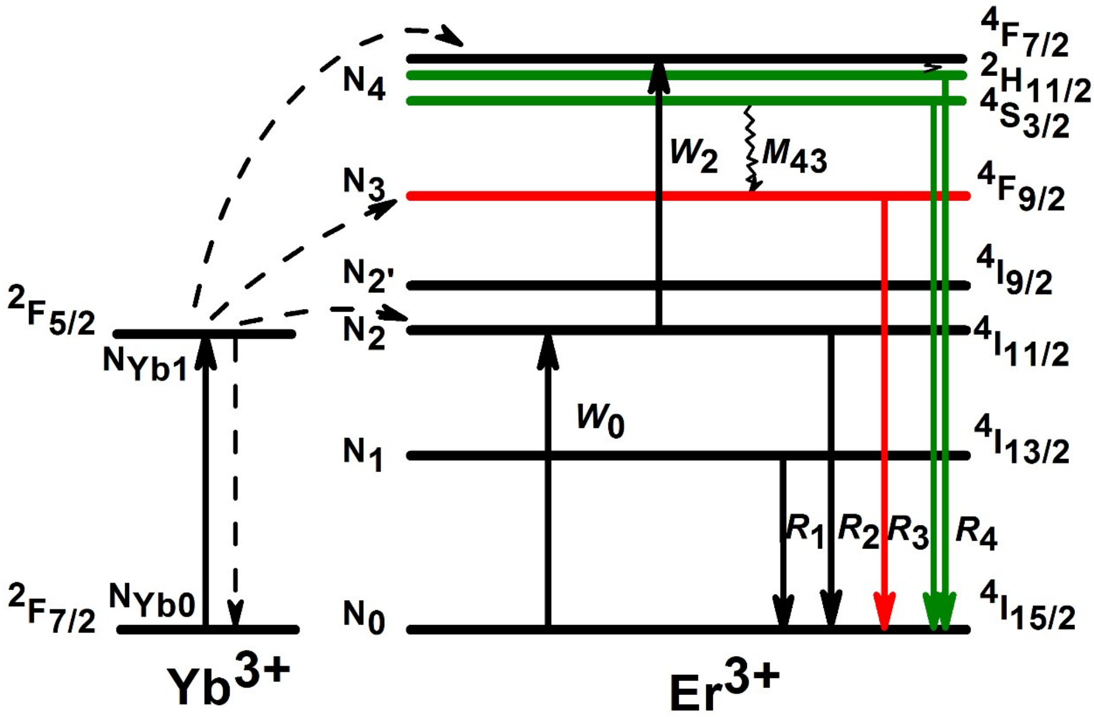

Fig. 21 Simplified energy-level diagrams illustrating the UC2 process.

$$\frac{dN_1}{dt} = -R_1N_1 \quad (14)$$

$$\frac{dN_2}{dt} = W_0N_{Yb1}N_0 - W_2N_{Yb1}N_2 - R_2N_2 \quad (15)$$

$$\frac{dN_3}{dt} = M_{43}N_4 - R_3N_3 \quad (16)$$

$$\frac{dN_4}{dt} = W_2N_{Yb1}N_2 - R_4N_4 \quad (17)$$

To solve the rate equations in stationary conditions, (14)~(17) convert to:

$$-R_1N_1 = 0 \quad (18)$$

$$W_0N_{Yb1}N_0 - W_2N_{Yb1}N_2 - R_2N_2 = 0 \quad (19)$$

$$M_{43}N_4 - R_3N_3=0 \quad (20)$$

$$W_2N_{Yb1}N_2 - R_4N_4 = 0 \quad (21)$$

According to (20), we obtain:

$$\frac{N_3}{N_4} = \frac{M_{43}}{A_3} \qquad (22)$$

UC3:

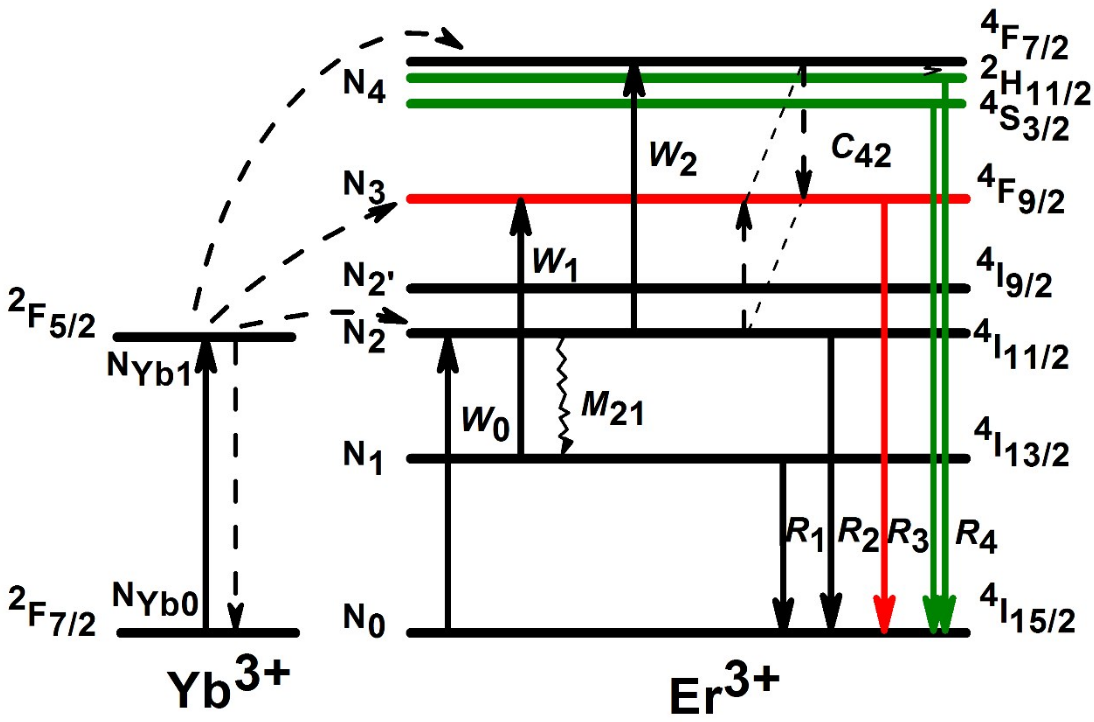

Fig. 22 Simplified energy-level diagrams illustrating the UC3 process.

$$\frac{dN_1}{dt} = M_{21}N_2 - W_1N_{Yb1}N_1 - R_1N_1 \quad (23)$$

$$\frac{dN_2}{dt} = W_0N_{Yb1}N_0 - M_{21}N_2 - W_2N_{Yb1}N_2 - C_{42}N_4N_2 - R_2N_2 \quad (24)$$

$$\frac{dN_3}{dt} = W_1N_{Yb1}N_1 + 2C_{42}N_4N_2 - R_3N_3 \quad (25)$$

$$\frac{dN_4}{dt} = W_2N_{Yb1}N_2 - C_{42}N_4N_2 - R_4N_4 \quad (26)$$

To solve the rate equations in stationary conditions, (23)~(26) convert to:

$$M_{21}N_2 - W_1N_{Yb1}N_1 - R_1N_1 = 0 \quad (27)$$

$$W_0N_{Yb1}N_0 - M_{21}N_2 - W_2N_{Yb1}N_2 - C_{42}N_4N_2 - R_2N_2 = 0 \quad (28)$$

$$W_1N_{Yb1}N_1 + 2C_{42}N_4N_2 - R_3N_3 = 0 \quad (29)$$

$W_2N_{Yb1}N_2 - C_{42}N_4N_2 - R_4N_4 = 0$ (30)

Considering that for UC3 the cross-relaxation process between N_2 and N_4 is the main population process for red emission, the population process W_1 is neglectable, moreover, the radiative rate of R_1 and R_2 can also be neglectable. Then (27)~(29) become:

$W_0N_{Yb1}N_0 - W_2N_{Yb1}N_2 - C_{42}N_4N_2 = 0$ (31)

$2C_{42}N_4N_2 - R_3N_3 = 0$ (32)

According to (32), we obtain:

$$\frac{N_3}{N_4} = \frac{2C_{42}N_2}{R_3} \quad (33)$$

According to (30), we obtain:

$$N_4 = \frac{W_2N_{Yb1}N_2}{C_{42}N_2 + R_4} \quad (34)$$

Inserting (34) to (28):

$$2C_{42}W_2{N_2}^2 + (W_2R_4 - C_{42}W_0N_0)N_2 - W_0N_0R_4 = 0 \quad (35)$$

According to (35), we get:

$$N_2 = \frac{C_{42}W_0N_0 - W_2R_4 + \sqrt{R_4^2W_2^2 + 6C_{42}W_2R_4W_0N_0 + C_{42}^2W_0^2N_0^2}}{4C_{42}W_2} \quad (36)$$

According to (33) and (36), we get:

$$\frac{N_3}{N_4} = \frac{-R_4W_2 + C_{42}W_0N_0}{2R_3W_2} + \frac{\sqrt{R_4^2W_2^2 + 6C_{42}W_2R_4W_0N_0 + C_{42}^2W_0^2N_0^2}}{2R_3W_2} \quad (37)$$

UC4:

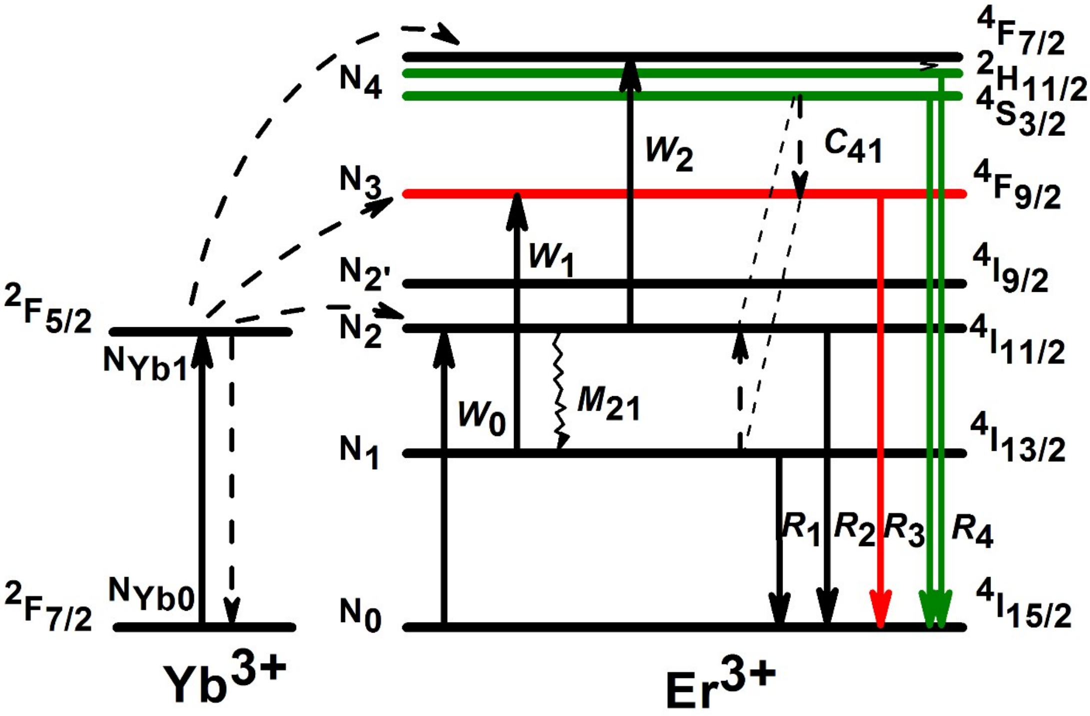

Fig. 23 Simplified energy-level diagrams illustrating the UC4 process.

$$\frac{dN_1}{dt} = M_{21}N_2 - C_{41}N_4N_1 - W_1N_{Yb1}N_1 - R_1N_1 \quad (38)$$

$$\frac{dN_2}{dt} = W_0N_{Yb1}N_0 + C_{41}N_4N_1 - M_{21}N_2 - W_2N_{Yb1}N_2 - R_2N_2 \quad (39)$$

$$\frac{dN_3}{dt} = W_1N_{Yb1}N_1 + C_{41}N_4N_1 - R_3N_3 \quad (40)$$

$$\frac{dN_4}{dt} = W_2N_{Yb1}N_2 - C_{41}N_4N_1 - R_4N_4 \quad (41)$$

To solve the rate equations in stationary conditions, (38)~(41) convert to:

$$M_{21}N_2 - C_{41}N_4N_1 - W_1N_{Yb1}N_1 - R_1N_1 = 0 \quad (42)$$

$$W_0N_{Yb1}N_0 + C_{41}N_4N_1 - M_{21}N_2 - W_2N_{Yb1}N_2 - R_2N_2 = 0 \quad (43)$$

$$W_1N_{Yb1}N_1 + C_{41}N_4N_1 - R_3N_3 = 0 \quad (44)$$

$W_2 N_{Yb1} N_2 - C_{41} N_4 N_1 - R_4 N_4 = 0$ (45)

Considering that for UC4 the cross-relaxation process between N_1 and N_4 is the main population process for red emission, the population process W_1 is neglectable, moreover, the radiative rate of R_1 and R_2 can also be neglectable. Then (42)~(44) become:

$M_{21} N_2 - C_{41} N_4 N_1 = 0$ (46)

$W_0 N_{Yb1} N_0 + C_{41} N_4 N_1 - M_{21} N_2 - W_2 N_{Yb1} N_2 = 0$ (47)

$C_{41} N_4 N_1 - R_3 N_3 = 0$ (48)

According to (48):

$$\frac{N_3}{N_4} = \frac{C_{41} N_1}{R_3} \quad (49)$$

(46)+(47):

$W_0 N_{Yb1} N_0 - W_2 N_{Yb1} N_2 = 0$ (50)

According to (50):

$$N_2 = \frac{W_0 N_0}{W_2} \quad (51)$$

(46)-(45):

$M_{21} N_2 - W_2 N_{Yb1} N_2 + R_4 N_4 = 0$ (52)

According to (52):

$$N_4 = \frac{(W_2 N_{Yb1} - M_{21})}{R_4} N_2 \quad (53)$$

According to (51) and (53):

$$N_4 = \frac{(W_2 N_{Yb1} - M_{21}) W_0 N_0}{R_4 \qquad W_2} \quad (54)$$

Inserting (51) and (54) into (46):

$$N_1 = \frac{M_{21} R_4}{C_{41}(W_2 N_{Yb1} - M_{21})} \quad (55)$$

Inserting (55) into (49):

$$\frac{N_3}{N_4} = \frac{R_4 M_{21}}{R_3 (W_2 N_{Yb1} - M_{21})} \quad (56)$$

UC5:

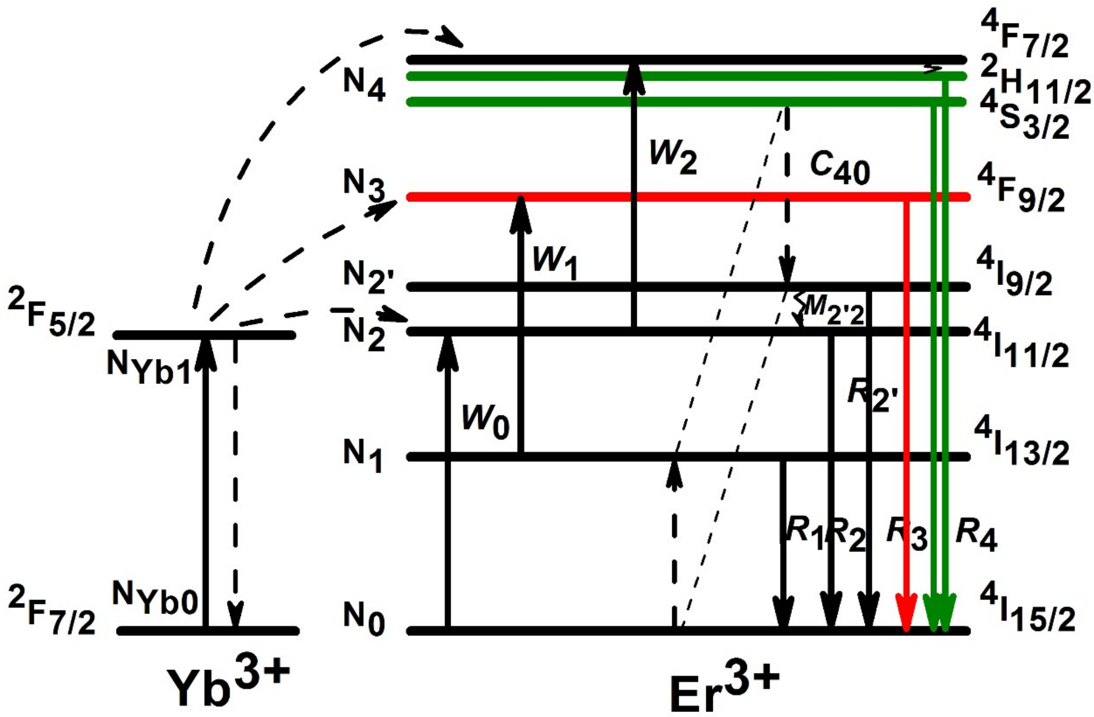

Fig. 24 Simplified energy-level diagrams illustrating the UC5 process.

$$\frac{dN_1}{dt} = C_{40}N_4N_0 - W_1N_{Yb1}N_1 - R_1N_1 \quad (57)$$

$$\frac{dN_2}{dt} = W_0N_{Yb1}N_0 + M_{2'2}N_{2'} - W_2N_{Yb1}N_2 - R_2N_2 \quad (58)$$

$$\frac{dN_{2'}}{dt} = C_{40}N_4N_0 - M_{2'2}N_{2'} - R_{2'}N_{2'} \quad (59)$$

$$\frac{dN_3}{dt} = W_1N_{Yb1}N_1 - R_3N_3 \quad (60)$$

$$\frac{dN_4}{dt} = W_2N_{Yb1}N_2 - C_{40}N_4N_0 - R_4N_4 \quad (61)$$

To solve the rate equations in stationary conditions, (57)~(61) convert to:

$$C_{40}N_4N_0 - W_1N_{Yb1}N_1 - R_1N_1 = 0 \quad (62)$$

$$W_0N_{Yb1}N_0 + M_{2'2}N_{2'} - W_2N_{Yb1}N_2 - R_2N_2 = 0 \quad (63)$$

$C_{40}N_4N_0 - M_{2'2}N_{2'} - R_{2'}N_{2'} = 0$ (64)

$W_1N_{Yb1}N_1 - R_3N_3 = 0$ (65)

$W_2N_{Yb1}N_2 - C_{40}N_4N_0 - R_4N_4 = 0$ (66)

Due to the radiative rate of R_1 and R_2 can be neglectable, then (62) become:

$C_{40}N_4N_0 - W_1N_{Yb1}N_1 = 0$ (67)

According to (67),

$$N_4 = \frac{W_1N_{Yb1}N_1}{C_{40}N_0} \quad (68)$$

According to (65),

$$N_3 = \frac{W_1N_{Yb1}N_1}{R_3} \quad (69)$$

According to (68) and (69),

$$\frac{N_3}{N_4} = \frac{C_{40}N_0}{R_3} \quad (70)$$

UC6:

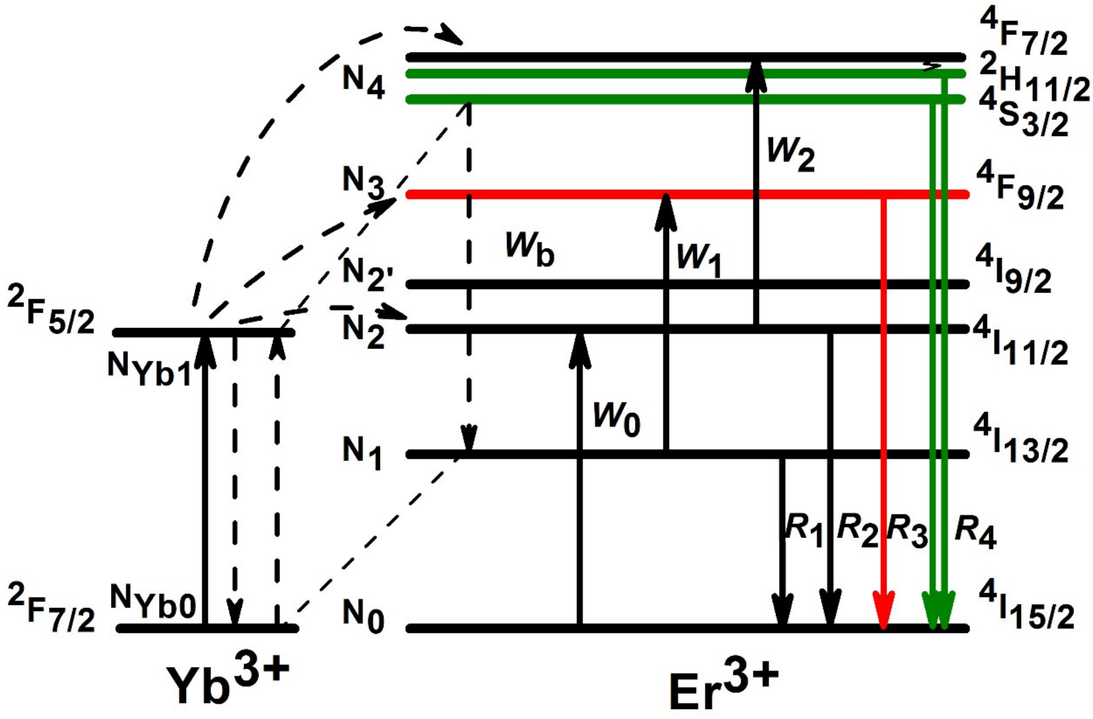

Fig. 25 Simplified energy-level diagrams illustrating the UC6 process.

$$\frac{dN_1}{dt} = W_b N_{Yb0} N_4 - W_1 N_{Yb1} N_1 - R_1 N_1 \quad (71)$$

$$\frac{dN_2}{dt} = W_0 N_{Yb1} N_0 - W_2 N_{Yb1} N_2 - R_2 N_2 \quad (72)$$

$$\frac{dN_3}{dt} = W_1 N_{Yb1} N_1 - R_3 N_3 \quad (73)$$

$$\frac{dN_4}{dt} = W_2 N_{Yb1} N_2 - W_b N_{Yb0} N_4 - R_4 N_4 \quad (74)$$

To solve the rate equations in stationary conditions, (71)~(74) convert to:

$$W_b N_{Yb0} N_4 - W_1 N_{Yb1} N_1 - R_1 N_1 = 0 \quad (75)$$

$$W_0 N_{Yb1} N_0 - W_2 N_{Yb1} N_2 - R_2 N_2 = 0 \quad (76)$$

$$W_1 N_{Yb1} N_1 - R_3 N_3 = 0 \quad (77)$$

$$W_2 N_{Yb1} N_2 - W_b N_{Yb0} N_4 - R_4 N_4 = 0 \quad (78)$$

Due to the radiative rate of R_1 and R_2 can be neglectable, then (75) become:

$$W_b N_{Yb0} N_4 - W_1 N_{Yb1} N_1 = 0 \quad (79)$$

According to (79):

$$N_4 = \frac{W_1 N_{Yb1} N_1}{W_b N_{Yb0}} \quad (80)$$

According to (77):

$$N_3 = \frac{W_1 N_{Yb1} N_1}{R_3} \quad (81)$$

According to (80) and (81):

$$\frac{N_3}{N_4} = \frac{W_b N_{Yb0}}{R_3} \quad (82)$$

UC7:

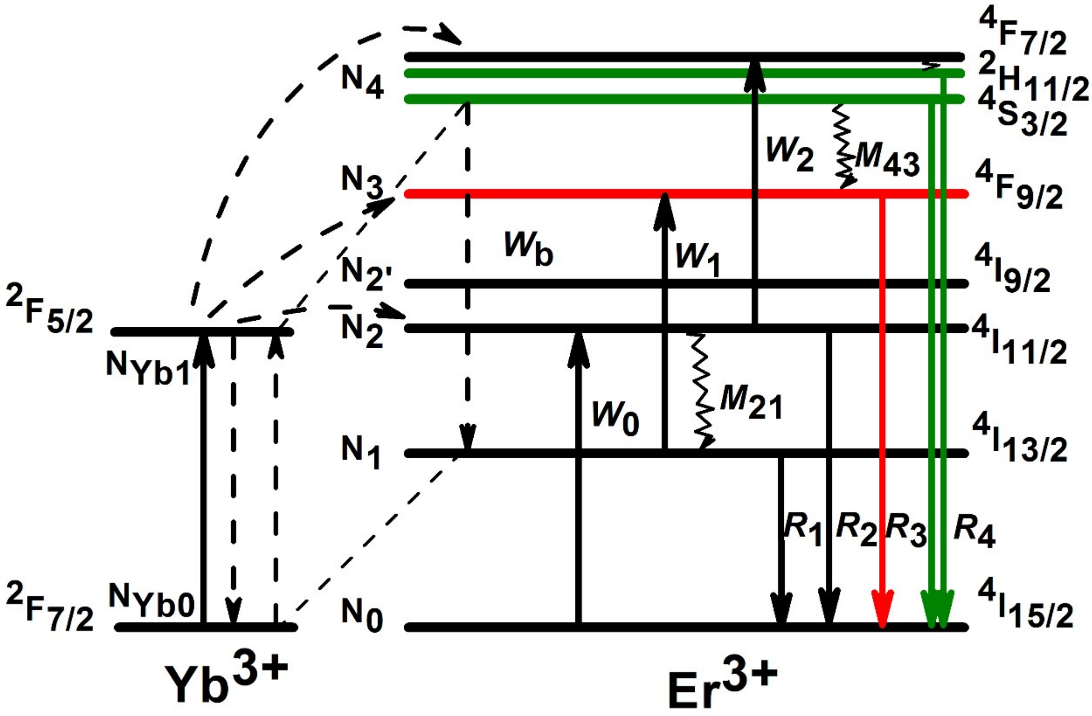

Fig. 26 Simplified energy-level diagrams illustrating the UC7 process.

$$\frac{dN_1}{dt} = W_b N_{Yb0} N_4 + M_{21} N_2 - R_1 N_1 \quad (83)$$

$$\frac{dN_2}{dt} = W_0 N_{Yb1} N_0 - W_2 N_{Yb1} N_2 - M_{21} N_2 - R_2 N_2 \quad (84)$$

$$\frac{dN_3}{dt} = W_1 N_{Yb1} N_1 + M_{43} N_4 - R_3 N_3 \quad (85)$$

$$\frac{dN_4}{dt} = W_2 N_{Yb1} N_2 - W_b N_{Yb0} N_4 - M_{43} N_4 - R_4 N_4 \quad (86)$$

To solve the rate equations in stationary conditions, (83)~(86) convert to:

$$W_b N_{Yb0} N_4 + M_{21} N_2 - R_1 N_1 = 0 \quad (87)$$

$$W_0 N_{Yb1} N_0 - W_2 N_{Yb1} N_2 - M_{21} N_2 - R_2 N_2 = 0 \quad (88)$$

$$W_1 N_{Yb1} N_1 + M_{43} N_4 - R_3 N_3 = 0 \quad (89)$$

$$W_2 N_{Yb1} N_2 - W_b N_{Yb0} N_4 - M_{43} N_4 - R_4 N_4 = 0 \quad (90)$$

According to (90):

$$\frac{N_2}{N_4} = \frac{W_2 N_{Yb1}}{W_b N_{Yb0} + M_{43} + R_4} \quad (91)$$

According to (87):

$$N_1 = \frac{W_b N_{Yb0} N_4}{R_1} + \frac{M_{21} N_2}{R_1} \quad (92)$$

According to (89):

$$N_3 = \frac{W_1 N_{Yb1} N_1}{R_3} + \frac{M_{43} N_4}{R_3} \quad (93)$$

Inserting (92) into (93):

$$N_3 = \left(\frac{W_1 W_b N_{Yb0} N_{Yb1}}{R_1 R_3} + \frac{M_{43}}{R_3} \right) N_4 + \frac{W_1 N_{Yb1} M_{21} N_2}{R_1 R_3} \quad (94)$$

According to (94):

$$\frac{N_3}{N_4} = \left(\frac{W_1 W_b N_{Yb0} N_{Yb1}}{R_1 R_3} + \frac{M_{43}}{R_3} \right) + \frac{W_1 N_{Yb1} M_{21} N_2}{R_1 R_3 N_4} \quad (95)$$

Inserting (91) into (95):

$$\frac{N_3}{N_4} = \frac{W_1 W_b N_{Yb0} N_{Yb1}}{R_1 R_3} + \frac{M_{43}}{R_3} + \frac{W_1 M_{21} (W_b N_{Yb0} + M_{43} + R_4)}{R_1 R_3 W_2} \quad (96)$$

Steady-state rate equations are established to quantitatively analyze the upconversion process according to previous reports.[1-6] We denote as N_0, N_1, N_2, $N_{2'}$, N_3, and N_4 the population densities of the $^4I_{15/2}$, $^4I_{13/2}$, $^4I_{11/2}$, $^4I_{9/2}$, $^4F_{9/2}$, $^4S_{3/2}/^2H_{11/2}/^4F_{7/2}$ states of Er^{3+} ions, N_{Yb0} and N_{Yb1} the population densities of the $^2F_{7/2}$, $^2F_{5/2}$ states of Yb^{3+} ions, respectively. W_0, W_1, W_2 represent the energy transfer rates form excited Yb^{3+} to Er^{3+}. M_{21}, M_{43}, and $M_{2'2}$ represent the multi-phonon relaxation rates from Er^{3+} $^4I_{11/2} \rightarrow {}^4I_{13/2}$ and Er^{3+} $^2H_{11/2}/^4S_{3/2} \rightarrow {}^4F_{9/2}$, and Er^{3+} $^4I_{9/2} \rightarrow {}^4I_{11/2}$ respectively. C_{40}, C_{41}, C_{42} represent the cross relaxation rates between Er^{3+}. W_b represent the back energy transfer rates from excited Er^{3+} to Yb^{3+}. R_1, R_2, $R_{2'}$, R_3 and R_4 represent the radiative rates of $^4I_{13/2}$, $^4I_{11/2}$, $^4I_{9/2}$, $^4F_{9/2}$, $^4S_{3/2}/^2H_{11/2}$ states of Er^{3+}, respectively. The above UC3-UC6 rate equations are established based on that more doping concentration of Yb^{3+} than that of Er^{3+}. Hence, many radiative and nonradiative processes, such as $N1$, $N2$ radiative emissions, back energy transfer from Er^{3+} $^4I_{11/2} \rightarrow {}^4I_{15/2}$ transition to Yb^{3+} $^2F_{7/2} \rightarrow {}^2F_{5/2}$ transition and so on, can be neglected.

The change rates of N_{Yb1} are:

$$\frac{dN_{Yb1}}{dt} = \rho\sigma_{Yb}N_{Yb0} - \sum W_i N_i N_{Yb1} - R_{Yb1}N_{Yb1} \tag{97}$$

where ρ is the excitation photon flux, which is linearly related to excitation power densities, σ_{Yb} is the absorption cross-section of Yb^{3+}, R_{Yb1} represent the radiative rates of $^2F_{5/2}$ state of Yb^{3+}. Under steady-state condition, N_{Yb1} can be expressed as:

$$N_{Yb1} = \frac{\rho\sigma_{Yb}N_{Yb0}}{\sum W_i N_i + R_{Yb1}} \propto \rho \tag{98}$$

Therefore, according to the rate equations in UC1~UC7, and Eqn. (98), we obtained the Table S1.

Table S1. R/G relationship of the upconversion process.

Upconversion Mechanism	R/G (N_3/N_4)	Power dependent R/G
UC1	$\frac{W_1M_{21}R_4}{W_2R_3(R_1 + W_1N_{Yb1})}$	$(a\rho + c)^{-1}$
UC2	$\frac{M_{43}}{A_3}$	ρ^0
UC3	$\frac{-R_4W_2 + C_{42}W_0N_0}{2R_3W_2} + \frac{\sqrt{R_4^2W_2^2 + 6C_{42}W_2R_4W_0}}{2R_3W_2}$	ρ^0
UC4	$\frac{R_4M_{21}}{R_3(W_2N_{Yb1} - M_{21})}$	$(\rho - c)^{-1}$
UC5	$\frac{C_{40}N_0}{R_3}$	ρ^0
UC6	$\frac{W_bN_{Yb0}}{R_3}$	ρ^0
UC7	$\frac{M_{43}}{R_3} + \frac{W_1M_{21}(W_bN_{Yb0} + M_{43} + R_4}{R_1R_3W_2}$	$a\rho^1 + b$

$$+\frac{W_1 W_b N_{Yb0} N_{Yb1}}{R_1 R_3}$$

Part III. References

1. D. Gao, X. Zhang, H. Zheng, W. Gao and E. He, *J. Alloys Compd.* , 2013, **554**, 395-399.
2. P. Salas, C. Angeles-Chavez, J. A. Montoya, E. De la Rosa, L. A. Diaz-Torres, H. Desirena, A. Martinez, M. A. Romero-Romo and J. Morales, *Opt. Mater.* , 2005, **27**, 1295-1300.
3. G. Chen, G. Somesfalean, Y. Liu, Z. Zhang, Q. Sun and F. Wang, *Phys. Rev. B*, 2007, **75**, 195204.
4. J. H. Zhang, Z. D. Hao, J. Li, X. Zhang, Y. S. Luo and G. H. Pan, *Light: Sci. Appl.*, 2015, **4**, e239.
5. D. Xu, C. Liu, J. Yan, S. Yang and Y. Zhang, *J. Phys. Chem. C* 2015, **119**, 6852-6860.
6. R. B. Anderson, S. J. Smith, P. S. May and M. T. Berry, *J. Phys. Chem. Lett.* , 2014, **5**, 36-42.